Gas-Phase Organometallic Kinetics. 2. Dissociative Substitution Kinetics of $Fe(CO)_2(C_2H_4)_3$ by Transient IR Absorption Spectrometry

Bruce H. Weiller[†] and Edward R. Grant*[‡]

Contribution from the Department of Chemistry, Baker Laboratory, Cornell University, Ithaca, New York 14853. *Received July 2, 1986*

Abstract: The transient gas-phase complexes, *cis*-$Fe(CO)_2(C_2H_4)_3$, *trans*-$Fe(CO)_2(C_2H_4)_3$, and $Fe(CO)(C_2H_4)_4$, are observed by time-resolved IR absorption spectrometry after pulsed laser photolysis of mixtures of $Fe(CO)_3(C_2H_4)_2$ and C_2H_4. The isomers of $Fe(CO)_2(C_2H_4)_3$ relax by two, parallel dissociative substitution pathways to reform $Fe(CO)_3(C_2H_4)_2$. From the CO and C_2H_4 dependencies of the observed reaction rates we obtain the 295 K unimolecular decay constants for *cis*-$Fe(CO)_2(C_2H_4)_3$ and *trans*-$Fe(CO)_2(C_2H_4)_3$, $3.6 \pm 0.9 \times 10^3$ and $1.2 \pm 0.4 \times 10^3$ s^{-1}, respectively. The ratios of the bimolecular rate constants for CO and C_2H_4 recombination with the coordinatively unsaturated species, $Fe(CO)_2(C_2H_4)_2$, are found to be ~400, favoring reaction with CO.

Organometallic complexes with olefins as ligands constitute a very important class of compounds. Many catalytic processes involve olefins as substrates (e.g., hydrogenation, isomerization, polymerization, metathesis, and hydroformylation)[1] and therefore must proceed via olefin coordination. The bonding in these complexes has been the subject of much research.[2] Particular interest has focussed on the most elementary such ligand, ethylene.[3] Its small size facilitates theoretical calculations and minimizes steric effects.[4]

Olefin complexes of $Fe(CO)_x$ are especially interesting. $Fe(CO)_5$ is a very efficient photocatalyst for olefin hydrogenation and isomerization.[5,6] Olefin–iron–carbonyl complexes are generally unstable, however, and thus present difficulties for kinetic study. For example, neat $Fe(CO)_4$(olefin) compounds decompose at room temperature,[7] while $Fe(CO)_3(olefin)_2$ complexes have not been isolated in the absence of excess olefin.[8] $Fe(CO)_2(C_2H_4)_3$ and $Fe(CO)(C_2H_4)_4$ are very short-lived and have only recently been observed in low-temperature matrices.[9] Work over the past few years has demonstrated the importance of $Fe(CO)_3(olefin)_2$ complexes in $Fe(CO)_5$/olefin catalysis.[8,9,10]

We are currently studying the gas-phase hydrogenation and isomerization of olefins as catalyzed by $Fe(CO)_5$.[6] Our focus is the fundamental kinetics of the elementary chemical reactions involved in these catalytic cycles. By working in the gas phase, we obtain results unobscured by interactions with solvent. We have recently investigated the gas-phase kinetics of the reaction[11]

$$Fe(CO)_3(C_2H_4)_2 + CO \rightarrow Fe(CO)_4(C_2H_4) + C_2H_4$$

a process that we have found competes with catalytic hydrogenation.

In this paper we examine the reactions of higher ethylene iron carbonyls. We report the first gas-phase observation of *cis*- and *trans*-$Fe(CO)_2(C_2H_4)_3$ and $Fe(CO)(C_2H_4)_4$ and present a kinetic study of the conversion of the isomers of $Fe(CO)_2(C_2H_4)_3$ to $Fe(CO)_3(C_2H_4)_2$ by microsecond time resolved, infrared absorption spectrometry. Our results show that *cis*- and *trans*-$Fe(CO)_2(C_2H_4)_3$, generated by photolysis of $Fe(CO)_3(C_2H_4)_2$ with excess C_2H_4, react with CO via separate, parallel dissociative substitution pathways to reform $Fe(CO)_3(C_2H_4)_2$. We obtain unimolecular decay constants for *cis*- and *trans*-$Fe(CO)_2(C_2H_4)_3$ and branching ratios for the reactions of unsaturated intermediates with CO relative to C_2H_4.

Experimental Section

The experimental apparatus is diagrammed in Figure 1. The technique of time-resolved IR absorption as applied to organometallics has recently been reviewed.[12] A pulsed UV excimer laser beam (Lambda Physik, EMG-201 MSC) crosses an incoherent IR beam in a static gas cell. A cylindrical lens ensures that the UV beam fills the 5 cm diameter cell. The IR source is a 2000 °C Nernst glower (Artcor) driven at 1 kHz to prevent thermal fluctuations. The IR beam is collimated by an off-axis parabolic mirror and focussed by a CaF_2 lens through the cell and onto the slits of a 0.3-m monochromator (Instruments SA, HR-320). Wavelengths are calibrated separately on DCl absorption features. The wavelength-resolved IR beam is focussed onto a 77 K InSb detector (Infrared Associates, 0.13 cm^2). A 4.5 μm long-wave pass filter (OCLI) removes higher order grating reflections. The detector, its matched preamplifier, and a low-pass filter (two-pole, Bessel) are all enclosed in a radio-frequency shield (Lingren Associates). The IR voltage signal is passed through an AC-coupled amplifier (Tektronix AM-502) and then to a 8-bit digital oscilloscope (Tektronix 468) for digitizing and averaging. The digitizer is triggered by the laser pulse with a photodiode. Averaged traces are passed to a laboratory computer (HP-85) followed by a minicomputer (Prime 9955) for storage and processing. High-resolution, single-beam IR spectra of the sample before and after irradiation are obtained by use of a chopper, lock-in amplifier, and chart recorder.

The bandwidth and wavelength resolution limits of the apparatus are

[†]Present address: Argonne National Laboratory, Chemistry Division, Argonne, Illinois 60439.

[‡]Address correspondence to this author at the Department of Chemistry, Purdue University, West Lafayette, Indiana 47907.

(1) Parshall, G. W. *Homogeneous Catalysis*; Wiley: New York, 1980.
(2) (a) Dewar, M. J. S. *Bull. Soc. Chim. Fr.* **1951**, *18*, C79. (b) Chatt, J.; Duncanson, L. A. *J. Chem. Soc.* **1953**, 2939. (c) Ittel, S. D.; Ibers, J. A. *Adv. Organomet. Chem.* **1976**, *14*, 33.
(3) (a) Elian, M.; Hoffmann, R. *Inorg. Chem.* **1975**, *14*, 1058. (b) Albright, T. A.; Hoffmann, R.; Thibeault, J. C.; Thorn, D. L. *J. Am. Chem. Soc.* **1979**, *101*, 3801. (c) Rosch, N.; Hoffmann, R. *Inorg. Chem.* **1974**, *13*, 2656. (d) Stockis, A.; Hoffmann, R. *J. Am. Chem. Soc.* **1980**, *102*, 2952 and references therein. (e) Bachman, C.; Demuynck, J.; Veillard, A. *J. Am. Chem. Soc.* **1978**, *100*, 2366. (f) Basch, H.; Newton, M. D.; Moskowitz, J. W. *J. Chem. Phys.* **1978**, *69*, 584. (g) Swope, W. L.; Schaefer, H. F., III *Mol. Phys.* **1977**, *34*, 1037. (h) Garcia-Prieto, J.; Novaro, O. *Mol. Phys.* **1980**, *41*, 205. (i) Kafafi, Z. H.; Hauge, R. H.; Margrave, J. L. *J. Am. Chem. Soc.* **1985**, *107*, 7550.
(4) Stainer, M. V. R.; Takats, J. *Inorg. Chem.* **1982**, *21*, 4044.
(5) (a) Asinger, F.; Fell, B.; Collin, G. *Chem. Ber.* **1963**, *96*, 716. (b) Asinger, F.; Fell, B.; Schrage, K. *Chem. Ber.* **1965**, *98*, 372, 381. (c) Carr, M. D.; Kane, V. V.; Whitting, M. C. *Proc. Chem. Soc., London* **1964**, 408. (d) Schroeder, M. A.; Wrighton, M. S. *J. Am. Chem. Soc.* **1976**, *98*, 551. (e) Schroeder, M. A.; Wrighton, M. S. *J. Organomet. Chem.* **1977**, *128*, 345. (f) Mitchener, J. C.; Wrighton, M. S. *J. Am. Chem. Soc.* **1981**, *103*, 975. (g) Chase, D. B.; Weigert, F. J. *J. Am. Chem. Soc.* **1981**, *103*, 977.
(6) (a) Whetten, R. L.; Fu, K.-J.; Grant, E. R. *J. Am. Chem. Soc.* **1982**, *104*, 4270. (b) Whetten, R. L.; Fu, K.-J.; Grant, E. R. *J. Chem. Phys.* **1983**, *79*, 2626. (c) Miller, M. E.; Grant, E. R. *Proc. SPIE* **1984**, *458*, 154. (d) Miller, M. E; Grant, E. R. *J. Am. Chem. Soc.* **1984**, *106*, 4635. (e) Miller, M. E.; Grant, E. R. *J. Am. Chem. Soc.* **1985**, *107*, 3386.
(7) Murdoch, H. D.; Weiss, E. *Helv. Chim. Acta* **1963**, 1588.
(8) Fleckner, H.; Grevels, F.-W.; Hess, D. *J. Am. Chem. Soc.* **1984**, *106*, 2027.
(9) Wuu, Y.-M.; Bentsen, J. G.; Brinkley, C. G.; Wrighton, M. S., manuscript submitted.
(10) Miller, M. E.; Grant, E. R., unpublished.
(11) Weiller, B. H.; Miller, M. E.; Grant, E. R. *J. Am. Chem. Soc.*, submitted for publication.
(12) Poliakoff, M.; Weitz, E. In *Advances in Organometallic Chemistry*; Stone, F. G. A., Ed.; Academic: New York, 1986; Vol. 25, p 277.
(13) Ouderkirk, A. J.; Weitz, E. *J. Chem. Phys.* **1983**, *79*, 1089.

0002-7863/87/1509-1051$01.50/0

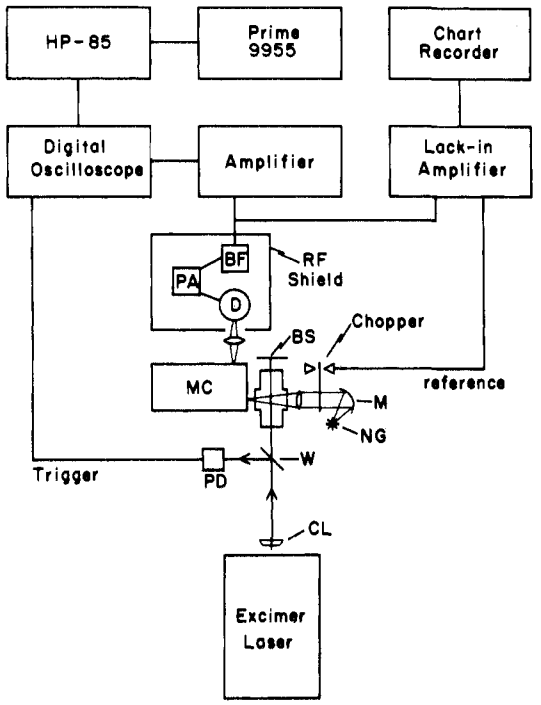

Figure 1. Experimental apparatus: CL = cylindrical lens; W = pyrex flat; NG = Nernst Glower; PD = photodiode; MC = monochromator; BS = beam stop; M = mirror; D = IR detector; PA = preamplifier; BF = band-pass filter. See text for details.

1 MHz and 0.5 cm^{-1}; however, better signal-to-noise is achieved at 30 kHz and 8-cm^{-1} resolution. The active IR path length is 3.3 cm. The laser wavelength, pulse width, and pulse energy are 351 nm, 10 ns, and 170 mJ, respectively. Thermal lens effects often observed in gas-phase, time-resolved, absorption spectrometry are not found here because the IR beam is much larger than the monochromator entrance slit.

As a check of the apparatus, we have been able to reproduce literature values[13] for the rate of recombination of $Fe(CO)_4$ with CO. For this a flow cell and rotameters (Fisher and Porter) for flow measurement were used.

$Fe(CO)_4(C_2H_4)$ is synthesized by the method of Murdoch and Weiss.[7] Mixtures of CO (Matheson, Research grade) and C_2H_4 (Matheson, CP grade, purified by 3 freeze–pump–thaw cycles) are prepared from known volumes. Reagent pressures are 0.30 Torr $Fe(CO)_4(C_2H_4)$, 0.30 to 1.3 Torr CO, and 200–800 Torr C_2H_4. Pressures are measured with either a capacitance manometer (MKS, 0–10 Torr) or Bourdon tube gauge (Heise, 0–50 psia). The temperature in all experiments is 295 K.

Results

The first step in the formation of $Fe(CO)_2(C_2H_4)_3$ and $Fe(CO)(C_2H_4)_4$ is the conversion of $Fe(CO)_4(C_2H_4)$ to metastable $Fe(CO)_3(C_2H_4)_2$ by photolysis in the presence of C_2H_4. The slow kinetics of $Fe(CO)_3(C_2H_4)_2 + CO \rightarrow Fe(CO)_4(C_2H_4) + C_2H_4$ have been discussed in detail.[11] The changes in the IR spectra as $Fe(CO)_4(C_2H_4)$ is photolyzed with C_2H_4 are shown in Figure 2. Complete conversion to $Fe(CO)_3(C_2H_4)_2$ (2069, 2001, and 1997 cm^{-1}) and CO is achieved with prolonged photolysis. Accurate knowledge of this native CO pressure is critical for kinetic analysis so the extent of conversion is carefully monitored. After complete conversion of $Fe(CO)_4(C_2H_4)$ to $Fe(CO)_3(C_2H_4)_2$ is achieved, then the infrared transients resulting from photolysis of $Fe(CO)_2(C_2H_4)_2$ are clearly discernable.

Transient waveforms are displayed as the change in absorbance with time referenced to zero at the laser pulse. Negative waveforms correspond to photolytic destruction of the initial $Fe(CO)_3(C_2H_4)_2$ species followed by subsequent reformation, while positive transients correspond to photoproduction of new species with subsequent decay.

Typical data are shown in Figure 3. We observe four distinct chemical species as evidenced by the four distinct waveforms observed at different wavelengths (1990, 1979, 1965, and 1954 cm^{-1}). At 1990 cm^{-1} (Figure 3a) is a shoulder of the most intense band of $Fe(CO)_3(C_2H_4)_2$. As expected, the laser pulse photolyzes

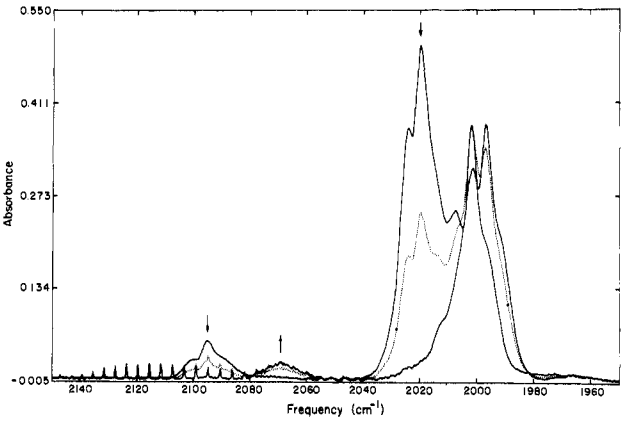

Figure 2. IR spectra as $Fe(CO)_4(C_2H_4)$ is photolyzed with C_2H_4. The arrows indicate growth or decay of bands with photolysis.

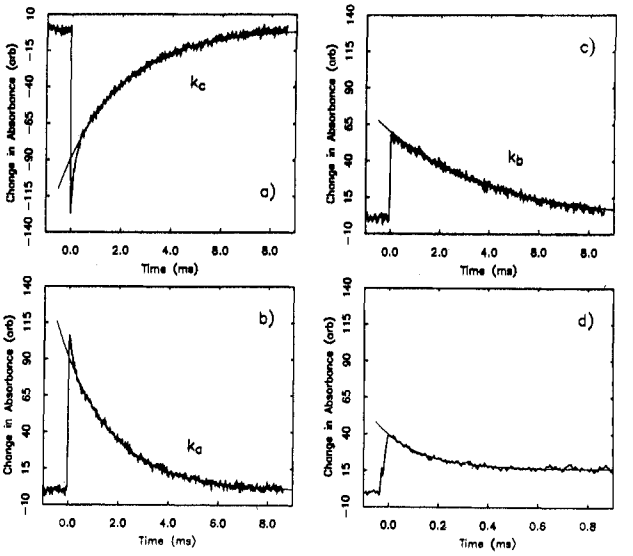

Figure 3. Typical IR transient waveforms: (a) 1990 cm^{-1}, (b) 1979 cm^{-1}, (c) 1965 cm^{-1}, and (d) 1954 cm^{-1}. The experimental conditions are 800 Torr C_2H_4, 0.30 Torr CO, and 0.30 Torr $Fe(CO)_4(C_2H_4)$ initially. All of the scales are the same except the abscissa in part d, which is expanded tenfold. The solid lines are the nonlinear least-squares exponential fits.

$Fe(CO)_3(C_2H_4)_2$, giving a negative waveform. The recovery is distinctly biexponential. Three new species (positive waveforms) are observed at lower frequencies. The 1979- and 1954-cm^{-1} (Figure 3, b and d) decays are biexponential while that at 1965 cm^{-1} (Figure 3c) is single exponential. The slow component at 1954 cm^{-1} matches the overall decay at 1965 cm^{-1}. The single exponential fits to the major decay (or rise) component at each wavelength are shown.

From a series of kinetic traces as in Figure 3, it is possible to reconstruct an infrared absorption spectrum of the sample as a function of time following irradiation. For this the resolution is increased to 5 cm^{-1}, and traces are taken every 4 cm^{-1} from 2017 to 1946 cm^{-1}. The traces are amplitude normalized relative to 1990 cm^{-1}. Point spectra are constructed by taking instantaneous amplitudes from each waveform at specific time intervals. A spline fit[14] is used to smooth the data. Results are shown in Figure 4, again as the change in absorbance. The wavelengths for the traces in Figure 3 are shown with arrows. All the wavelengths monitored are indicated on the abscissa. The four species mentioned above are also evident here by polarity and temporal behavior. Of note is the isobestic point at 1985 cm^{-1} and an additional small, fast, reproducible feature at 2017 cm^{-1} that is unidentified.

The slow exponentials at 1990, 1979, and 1965 cm^{-1} display strong CO and C_2H_4 dependencies. Figure 5 shows that the best

(14) IMSL subroutine ICSCCU, International Mathematics and Statistics Library, Inc.

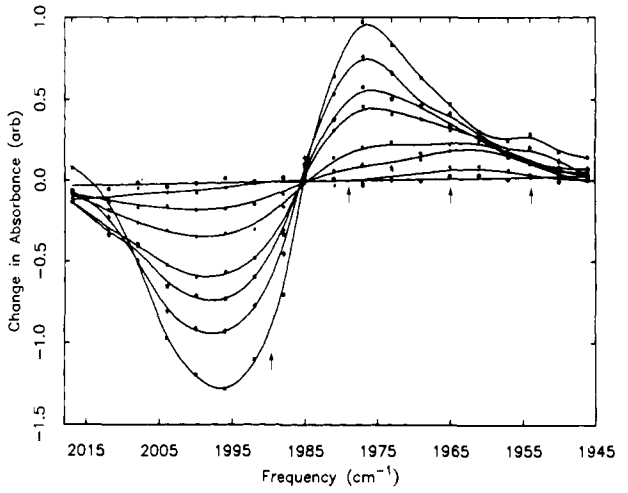

Figure 4. Transient IR absorption spectrum. Constructed from traces as in Figure 3. The resolution is 5 cm^{-1} and the traces are taken every 4 cm^{-1}. The points are the data and the solid lines are smoothed spline fits. The times of the spectra after the laser pulse are 30 μs, 225 μs, 616 μs, 1.01 ms, 2.33 ms, 3.62 ms, 6.12 ms, and 8.68 ms. The arrows indicate the wavelengths for the traces in Figure 3.

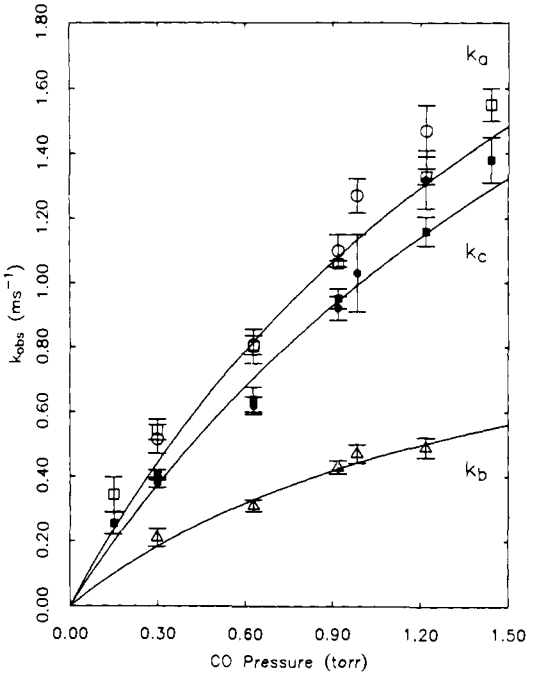

Figure 5. CO pressure dependence of the observed decay constants. Points are ○, □ = 1979 cm^{-1}; ●, ■ = 1990 cm^{-1}; △ = 1965 for the exponential fits as in Figure 3. The solid lines are fits to the function in eq 1.

fit exponential decay constants (k_{obsd}) are a function of CO pressure at constant C_2H_4 pressure (800 Torr). The CO pressure reported includes the contribution of 0.30 Torr released by photolysis of $Fe(CO)_4(C_2H_4)$. The points at 0.15 Torr CO are obtained by starting with 0.15 Torr $Fe(CO)_4(C_2H_4)$. Each point represents the average of at least six independent experiments and accompanying temporal fits. The solid line is the best weighted nonlinear least-squares fit[15] to the expression

$$k_{obsd} = \frac{P(CO)}{Q + (CO)} \quad (1)$$

The slow exponentials at 1990, 1979, and 1965 cm^{-1} also display inverse dependencies on C_2H_4. Figure 6 shows a plot of the inverse of k_{obsd} for 1979 cm^{-1} against C_2H_4 pressure at constant CO pressure (0.90 Torr). Again each point is the average of at least six independent experiments and fits. The solid line is the weighted

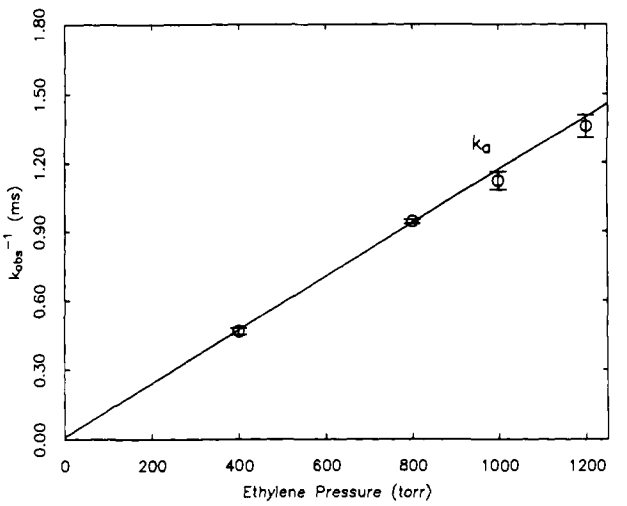

Figure 6. C_2H_4 pressure dependence of the observed decay constant at 1979 cm^{-1}. The solid line is linear fit.

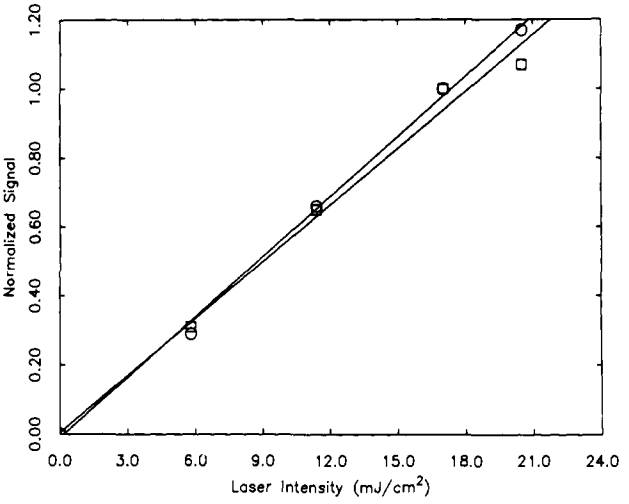

Figure 7. Dependence of signal amplitudes on laser intensity. The points are □ = 1990 cm^{-1} =, ○ = 1979 cm^{-1}. The solid lines are linear fits.

Table I. C_2H_4 and CO Pressure Dependences of Observed Decay Constants

	C_2H_4 (Torr)	CO (Torr)	k_a (ms^{-1})[a]	k_b (ms^{-1})	k_c (ms^{-1})
1	800	0.15	0.34 ± 0.05		0.25 ± 0.03
2	800	0.30	0.54 ± 0.03		0.40 ± 0.02
3	800	0.30	0.52 ± 0.04	0.21 ± 0.03	0.38 ± 0.02
4	800	0.63	0.80 ± 0.05		0.64 ± 0.04
5	800	0.63	0.81 ± 0.03	0.31 ± 0.02	0.62 ± 0.03
6	800	0.92	1.06 ± 0.07		0.95 ± 0.03
7	800	0.92	1.10 ± 0.05	0.43 ± 0.02	0.92 ± 0.04
8	800	0.99	1.27 ± 0.05	0.47 ± 0.03	1.03 ± 0.12
9	800	1.22	1.33 ± 0.02		1.16 ± 0.05
10	800	1.22	1.47 ± 0.08	0.49 ± 0.03	1.32 ± 0.09
11	800	1.44	1.55 ± 0.05		1.38 ± 0.07
12	400	0.30	0.92 ± 0.01		0.70 ± 0.02
13	400	0.30	0.96 ± 0.03	0.42 ± 0.01	0.66 ± 0.02
14	400	0.92	2.14 ± 0.06		2.01 ± 0.04
15	1000	0.92	0.90 ± 0.03		0.76 ± 0.03
16	1200	0.92	0.73 ± 0.03		0.56 ± 0.02

[a] Error limits are standard deviations obtained following measurements for no fewer than six replicate samples at each composition.

linear least-squares fit.[15] Although not shown, the decay at 1965 cm^{-1} is also inversely dependent on C_2H_4 (Table I, entry numbers 3 and 13). Signal intensities are observed to scale linearly with parent concentration at low $Fe(CO)_4(C_2H_4)$ partial pressure (<0.5

(15) Bevington, P. R. *Data Reduction and Error Analysis for the Physical Sciences*; McGraw-Hill: New York, 1969.

Table II. Power Dependence of Observed Decay Constants

	laser intensity (mJ/cm²)	k_a (ms⁻¹)	k_c (ms⁻¹)
1	5.8	0.53 ± 0.03	0.43 ± 0.02
2	11.4	0.52 ± 0.01	0.39 ± 0.01
3	17.0	0.47 ± 0.06	0.34 ± 0.01
4	20.5	0.51 ± 0.01	0.38 ± 0.01

Torr). Added buffer gas has no effect on k_{obsd} under our experimental conditions.

Finally, power dependencies of the signals at 1990 and 1979 cm^{-1} are shown in Figure 7. The amplitudes at each wavelength are linear with laser intensity, while the decay constants are independent of laser intensity (Table II).

Discussion

An immediate concern is the identity of the transient species formed upon photolysis of $Fe(CO)_3(C_2H_4)_2$ with C_2H_4. When CO is replaced by a less electron withdrawing ligand, such as C_2H_4, one expects a shift in the carbonyl IR bands to lower frequency[16] as we observe. We rule out unsaturated species on the basis of the long time scale over which each is observed[17] and the inverse dependence of their decay rates on C_2H_4 pressure. It is therefore likely that the transients are 18-electron complexes with three or more ethylene ligands. The linear power dependence of signal amplitudes and power independence of k_{obsd} exclude dinuclear complexes formed by recombination of unsaturated photoproducts. Dinuclear complexes of photoproducts with parent are also unlikely candidates owing to the observed linear dependence of signal amplitudes on parent density.

Our specific assignment is aided by recent matrix isolation work by Wuu et al.[9] They have assigned matrix IR absorptions at 1998 and 1955 cm^{-1} to *cis*-$Fe(CO)_2(C_2H_4)_3$ (**1a** or **1b**), 1942 cm^{-1} to *trans*-$Fe(CO)_2(C_2H_4)_3$ (**2**), and 1952 cm^{-1} to $Fe(CO)(C_2H_4)_4$.

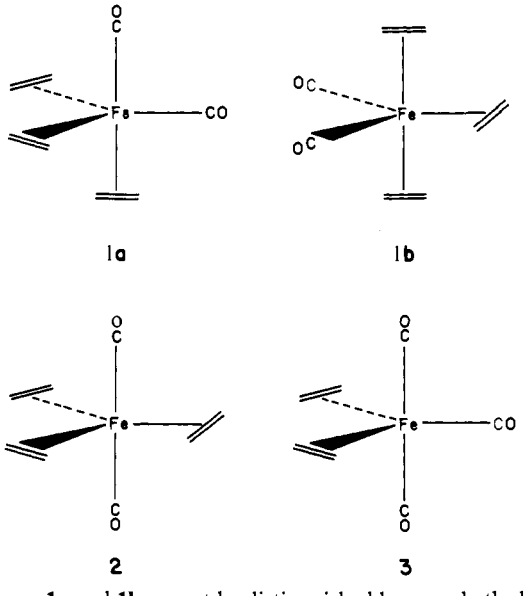

Structures **1a** and **1b** cannot be distinguished because both should have two carbonyl bands.[18] The structure shown for $Fe(CO)_3(C_2H_4)_2$ (**3**) is deduced from the number of infrared bands observed, together with comparison with known compounds and theoretical expectations.[11,3d] The appearance of successive sets of bands in the matrix spectra gives relative stabilities. These are assigned as[9]

$$Fe(CO)_3(C_2H_4)_2 \gg \textit{trans}\text{-}Fe(CO)_2(C_2H_4)_3 > \textit{cis}\text{-}Fe(CO)_2(C_2H_4)_3 > Fe(CO)(C_2H_4)_4$$

Table III. Assignment of Transient Absorptions

complex	freq (cm⁻¹)[a]
$Fe(CO)_3(C_2H_4)_2$	1997
cis-$Fe(CO)_2(C_2H_4)_3$	1976
trans-$Fe(CO)_2(C_2H_4)_3$	1965
$Fe(CO)(C_2H_4)_4$	1954

[a] ±5 cm^{-1}. [b] Matrix data predict that the high-frequency band of *cis*-$Fe(CO)_2(C_2H_4)_3$ will be obscured in our system by the strong $Fe(CO)_3(C_2H_4)_2$ peak.

Adopting a consistent set of gas-matrix spectral shifts and this stability series we tentatively assign our gas-phase transients as shown in Table III. We now turn to the kinetics for confirmation of this assignment.

From our work on $Fe(CO)_3(C_2H_4)_2$[11] and the work of others[19] on iron carbonyl complexes, we can expect dissociative substitution processes to carry the species assigned as *cis*-$Fe(CO)_2(C_2H_4)_3$ and *trans*-$Fe(CO)_2(C_2H_4)_3$ to $Fe(CO)_3(C_2H_4)_2$. Alternative mechanisms involving sequential conversion by either isomerization or substitution are excluded immediately on the basis of the following observations: (1) All of the observed decay constants are CO and C_2H_4 dependent, and (2) all rise times are electronically limited (3×10^4 s^{-1}). A rate increasing with CO pressure could signify either attack on the saturated reactant or reaction with its dissociation product. The fact that observed rates uniformly *decrease* with increasing C_2H_4 pressure, however, demands a preceding step of reversible ethylene decoordination. The simplest mechanism consistent with all of these observed facts is conventional dissociative substitution

$$\underset{\textbf{1a or 1b}}{\textit{cis}\text{-}Fe(CO)_2(C_2H_4)_3} \underset{k_2}{\overset{k_1}{\rightleftharpoons}} Fe(CO)_2(C_2H_4)_2 + C_2H_4$$

$$Fe(CO)_2(C_2H_2)_2 + CO \xrightarrow{k_3} \underset{\textbf{3}}{Fe(CO)_3(C_2H_4)_2}$$

$$\underset{\textbf{2}}{\textit{trans}\text{-}Fe(CO)_2(C_2H_4)_3} \underset{k_5}{\overset{k_4}{\rightleftharpoons}} Fe(CO)_2(C_2H_4)_2'$$

$$Fe(CO)_2(C_2H_4)_2' + CO \xrightarrow{k_6} \underset{\textbf{3}}{Fe(CO)_3(C_2H_4)_2}$$

where for the present we shall consider $Fe(CO)_2(C_2H_4)_2$ and $Fe(CO)_2(C_2H_4)_2'$ distinct isomers.

Applying the steady state assumption to $[Fe(CO)_2(C_2H_4)_2]$ and $[Fe(CO)_2(C_2H_4)_2']$ gives simple forms of the decay rates of *cis*-$Fe(CO)_2(C_2H_4)_3$ and *trans*-$Fe(CO)_2(C_2H_4)_3$.

$$-\frac{d[\textit{cis}\text{-}Fe(CO)_2(C_2H_4)_3]}{dt} = \frac{k_1k_3[CO][\textit{cis}\text{-}Fe(CO)_2(C_2H_4)_3]}{k_2[C_2H_4] + k_3[CO]} = k_a[\textit{cis}\text{-}Fe(CO)_2(C_2H_4)_3] \quad (2)$$

$$-\frac{d[\textit{trans}\text{-}Fe(CO)_2(C_2H_4)_3]}{dt} = \frac{k_4k_6[CO][\textit{trans}\text{-}Fe(CO)_2(C_2H_4)_3]}{k_5[C_2H_4] + k_6[CO]} = k_b[\textit{trans}\text{-}Fe(CO)_2(C_2H_4)_3] \quad (3)$$

(16) Purcell, K. F.; Kotz, J. C. *Inorganic Chemistry*; W. B. Saunders Co.: Philadelphia, 1977; p 904.

(17) Gas-phase bimolecular rate constants for CO recombination with unsaturated intermediates are on the order of 10^{10} M^{-1} s^{-1} when there is no spin change involved. For example, see: Ouderkirk, A. J.; Wermer, P.; Schultz, N. L.; Weitz, E. *J. Am. Chem. Soc.* **1983**, *105*, 3354. Ouderkirk, A. J.; Seder, T. A.; Weitz, E. *SPIE Proc.* **1984**, *458*, 148. Seder, T. A.; Church, S. P.; Ouderkirk, A. J.; Weitz, E. *J. Am Chem. Soc.* **1985**, *107*, 1432. Fletcher, T. R.; Rosenfeld, R. N. *J. Am. Chem. Soc.* **1985**, *107*, 2203. Fletcher, T. R.; Rosenfeld, R. N. *J. Am. Chem. Soc.* **1986**, *108*, 1686. Even when formally spin forbidden, the reactions are much faster (10^8 M^{-1} s^{-1}) than we observe (ref 13).

(18) Cotton, F. A. *Chemical Applications of Group Theory*; Wiley: New York, 1971. Wuu et al. calculate a OC–M–CO angle of 82° from the relative intensities of the IR bands of their matrix-isolated *cis*-$Fe(CO)_2(C_2H_4)_3$ (ref 9).

(19) (a) Angelici, R. J. *Organomet. Chem. Rev.* **1968**, *3*, 173. (b) Howell, J. A. S.; Burkinshaw, P. M. *Chem. Rev.* **1983**, *83*, 557. (c) Cardaci, G.; Narciso, V. *J. Chem. Soc., Dalton Trans.* **1972**, 2289. (d) Burkinshaw, P. M.; Dixon, D. T.; Howell, J. A. S. *J. Chem. Soc., Dalton Trans.* **1980**, 999. (e) Cardaci, G. *Inorg. Chem.* **1974**, *13*, 2974. (f) Cardaci, G. *Inorg. Chem.* **1974**, *13*, 368. (g) Cardaci, G. *Int. J. Chem. Kinet.* **1973**, *5*, 805. (h) Cardaci, G. *J. Organomet. Chem.* **1974**, *76*, 385.

In our experiments we estimate that no more than 1% of $Fe(CO)_3(C_2H_4)_2$ is photolyzed, so the excess concentrations of [CO] and $[C_2H_4]$ can be taken to be constant, and eq 2 and 3 can be simply integrated to give

$$[cis\text{-}Fe(CO)_2(C_2H_4)_3] = [cis\text{-}Fe(CO)_2(C_2H_4)_3]_0 \exp(-k_a t) \quad (4)$$

$$[trans\text{-}Fe(CO)_2(C_2H_4)_3] = [trans\text{-}Fe(CO)_2(C_2H_4)_3]_0 \exp(-k_b t) \quad (5)$$

where k_a and k_b are the CO and C_2H_4 dependent constants in eq 2 and 3. Mass balance gives the time dependence of product.

$$[Fe(CO)_3(C_2H_4)_2] = [Fe(CO)_3(C_2H_4)_2]_0 + [cis\text{-}Fe(CO)_2(C_2H_4)_3]_0 [1 - \exp(-k_a t)] + [trans\text{-}Fe(CO)_2(C_2H_4)_3]_0[1 - \exp(-k_b t)] \quad (6)$$

The above analysis predicts single exponential decays for both *cis*-$Fe(CO)_2(C_2H_4)_3$ and *trans*-$Fe(CO)_2(C_2H_4)_3$. Neglecting the small fast component on *cis*-$Fe(CO)_2(C_2H_4)_3$, both traces for *cis*-$Fe(CO)_2(C_2H_4)_3$ and *trans*-$Fe(CO)_2(C_2H_4)_3$ are well fit by single exponentials (Figure 3). Our analysis also predicts a biexponential recovery for $Fe(CO)_3(C_2H_4)_2$ (eq 6) with time constants identical with those for *cis*-$Fe(CO)_2(C_2H_4)_3$ and *trans*-$Fe(CO)_2(C_2H_4)_3$. The recovery of $Fe(CO)_3(C_2H_4)_2$ does contain a small fast component. This rise, however, is faster than the decay of either observed isomer of $Fe(CO)_2(C_2H_4)_3$ and thus must reflect a minor contribution from some other source of $Fe(CO)_3(C_2H_4)_2$.[20] The main component of the $Fe(CO)_3(C_2H_4)_2$ rise exhibits time constants that always lie intermediate between those of *cis*-$Fe(CO)_2(C_2H_4)_3$ and *trans*-$Fe(CO)_2(C_2H_4)_3$. For given conditions this wave form can easily be fit by a simple linear combination of the two reactant decays. Alternatively, for $k_a \simeq k_b$ eq 6 is approximated by

$$[Fe(CO)_3(C_2H_4)_2] = [Fe(CO)_3(C_2H_4)_2]_0 + \{[cis\text{-}Fe(CO)_2(C_2H_4)_3]_0 + [trans\text{-}Fe(CO)_2(C_2H_4)_3]_0\}[1 - \exp(k_c t)] \quad (7)$$

where k_c is a phenomenological rate constant determined by the average of k_a and k_b weighted by relative concentrations.

The mechanism above requires that k_a, k_b, and k_c all depend on both CO and C_2H_4 pressures, with explicit forms for k_a and k_b:

$$k_a = \frac{k_1 k_3[CO]}{k_2[C_2H_4] + k_3[CO]} \qquad k_b = \frac{k_4 k_6[CO]}{k_5[C_2H_4] + k_6[CO]} \quad (8)$$

Figure 5 shows the CO dependence of k_a and k_b. These data exhibit good fits to the functional forms of eq 8.

Equation 8 can be rearranged to a form linear in ethylene pressure:

$$\frac{1}{k_a} = \frac{1}{k_1} + \frac{k_2[C_2H_4]}{k_1 k_3[CO]} \qquad \frac{1}{k_b} = \frac{1}{k_4} + \frac{k_5[C_2H_4]}{k_4 k_6[CO]} \quad (9)$$

Figure 6 shows the C_2H_4 dependence of k_a^{-1}, together with a good linear fit in correspondence with eq 9.[21] Inverse dependence of k_b on $[C_2H_4]$ is also observed (Table I, entry numbers 3 and 13).

(20) Kinetic spectroscopy does not distinguish between cis isomers **1a** and **1b**. Wrighton and co-workers assign the **1a** structure to the *cis*-$Fe(CO)_2(C_2H_4)_3$ formed in their matrix system (see ref 9 and 18). The fast component in our decay at 1979 cm^{-1} and recovery at 1990 cm^{-1} could reflect the transformation of the less stable *cis*-$Fe(CO)_2(C_2H_4)_3$.

(21) Samples with composition nearest the intercept in this plot exhibit slight long-term sample decomposition (clustering). Over time under such low substrate concentration conditions, iron products deposit on the cell walls liberating CO. While this process appears not to affect the elementary sequence of gas-phase reactions (IR spectra are unchanged), the small amount of extra CO increases k_{obsd}, thereby artificially depressing the $(k_{obsd})^{-1}$ vs. $[C_2H_4]$ intercept. As noted in the text, kinetic fits of the ethylene dependence at higher ethylene pressures or with added CO agree well with data extracted from CO dependence plots.

Table IV. Derived Rate Constants

	unimolecular decay $(s^{-1})^a$	branching ratio[b]
$Fe(CO)_3(C_2H_4)_2$[c]	$2.9 \pm 0.3 \times 10^{-3}$	35 ± 5
trans-$Fe(CO)_2(C_2H_4)_3$	$1.2 \pm 0.4 \times 10^{+3}$	480 ± 220
cis-$Fe(CO)_2(C_2H_4)_3$	$3.6 \pm 0.9 \times 10^{+3}$	370 ± 130

[a] k_1 for *cis*-$Fe(CO)_2(C_2H_4)_3$ and k_4 for *trans*-$Fe(CO)_2(C_2H_4)_3$. [b] Ratio of bimolecular rate constants for reaction of the 16-electron precursor with CO relative to C_2H_4. In terms of rate constants these are for *trans*-$Fe(CO)_2(C_2H_4)_3$, k_6/k_4, and for *cis*-$Fe(CO)_2(C_2H_4)_3$, k_3/k_2. [c] Reference 11, at a temperature of 297 K.

Clearly, the time/concentration dependencies of the transient signals are consistent with our spectral assignments and proposed kinetic mechanism. Analysis of the data in terms of eq 8 and 9 yields explicit kinetic parameters. For example, note that over the range of the present experiments $[C_2H_4]/[CO]$ varies from 5330 to 570, yet in Figure 5 we easily see curvature that indicates the onset of saturation in [CO]. Thus by inspection we can immediately conclude that $k_2 \gg k_3$ and $k_5 \gg k_6$. More specifically, from the parameters of the nonlinear least-squares fit of the CO dependence of k_{obsd} for *cis*-$Fe(CO)_2(C_2H_4)_3$ (k_a) and *trans*-$Fe(CO)_2(C_2H_4)_3$ (k_b), we obtain quantitative unimolecular decay constants for *cis*-$Fe(CO)_2(C_2H_4)_3$ (k_1) and *trans*-$Fe(CO)_2(C_2H_4)_3$ (k_4) and the branching ratios for the reactions of the coordinatively unsaturated intermediates, $Fe(CO)_2(C_2H_4)_2$ and $Fe(CO)_2(C_2H_4)_2'$, with CO relative to C_2H_4 (k_3/k_2 and k_6/k_5, respectively). These are presented in Table IV together with analogous values derived for $Fe(CO)_3(C_2H_4)_2$ and $Fe(CO)_3(C_2H_4)$. The $Fe(CO)_2(C_2H_4)_3$ values from the variation of k_{obsd} with CO can be cross-checked with the ethylene dependence data. From the slope of $1/k_a$ vs. $[C_2H_4]$ (Figure 6), a value of $k_1k_3/k_2 = 940$ ms^{-1} is found. The CO dependence data yield a value of $k_1k_3/k_2 = 1330 \pm 570$ ms^{-1}. Similarly, from $1/k_b$ vs. $[C_2H_4]$ (Table I, entries 3 and 13), $k_4k_6/k_5 = 560$ ms^{-1} while the CO data give $k_4k_6/k_5 = 580 \pm 330$ ms^{-1}. This internal consistency of the numerical results further supports the validity of the kinetic mechanism and confirms our spectral assignments.

As a test, we have considered a subtle difference in which $Fe(CO)_2(C_2H_4)_2$ and $Fe(CO)_2(C_2H_4)_2'$ are the same intermediate. The coupled differential equations resulting when the steady state approximation is applied to this single intermediate have been integrated numerically by using reasonable values for the various rate constants. We find that such a scheme cannot reproduce the experimental data. Specifically, the large difference between time constants for *cis*-$Fe(CO)_2(C_2H_4)_3$ and *trans*-$Fe(CO)_2(C_2H_4)_3$ cannot be simulated while at the same time maintaining the similarity between time constants for *cis*-$Fe(CO)_2(C_2H_4)_3$ and $Fe(CO)_3(C_2H_4)_2$.

The proposal of distinct isomers of $Fe(CO)_2(C_2H_4)_2$ on the time scale of our experiment is not without precedent. High barriers to ethylene rotation which prevent isomerization have been calculated.[3a] Experimental evidence is present in very recent matrix isolation studies. Wuu et al. observe matrix infrared bands assigned to the cis isomer of unsaturated $Fe(CO)_2(C_2H_4)_2$.[9] The trans isomer is apparently absent, due perhaps to matrix perturbations that block its formation. Interestingly, they find *cis*-$Fe(CO)_2(C_2H_4)_3$ but no *trans*-$Fe(CO)_2(C_2H_4)_3$ following low-temperature irradiation of $Fe(CO)_3(C_2H_4)_2$. *trans*-$Fe(CO)_2(C_2H_4)_3$ is formed by subsequent chemical reactions as the matrix is warmed. This specificity in initial cis-only product formation is consistent with our proposal of separate isomers of unsaturated $Fe(CO)_2(C_2H_4)_2$ with distinct, stereospecific reactivities.

Acknowledgment. We thank C. G. Brinkley and M. S. Wrighton for communicating their results prior to publication. Acknowledgement is made to the donors of the Petroleum Research Fund, administered by the American Chemical Society, for support of this research.